Unraveling the H₂ Promotional Effect on Palladium-Catalyzed CO Oxidation Using a Combination of Temporally and Spatially Resolved Investigations

Caomhán Stewart,[†] Emma K. Gibson,*[‡,§] Kevin Morgan,*[†] Giannantonio Cibin,[‖] Andrew J. Dent,[‖] Christopher Hardacre,[⊥] Evgenii V. Kondratenko,[#] Vita A. Kondratenko,[#] Colin McManus,[†] Scott Rogers,[§,∇] Cristina E. Stere,[⊥] Sarayute Chansai,[⊥] Yi-Chi Wang,[&] Sarah J. Haigh,[&] Peter P. Wells,[§,‖,○] and Alexandre Goguet[†]

[†]School of Chemistry and Chemical Engineering, Queen's University Belfast, Stranmillis Road, Belfast BT9 5AG, U.K.

[‡]School of Chemistry, Joseph Black Building, University of Glasgow, Glasgow G12 8QQ, U.K.

[§]UK Catalysis Hub, Research Complex at Harwell, Didcot, Oxfordshire OX11 0FA, U.K.

[‖]Diamond Light Source Ltd, Harwell Science & Innovation Campus, Didcot, Oxfordshire OX11 0DE, U.K.

[⊥]School of Chemical Engineering and Analytical Science, University of Manchester, Manchester M13 9PL, U.K.
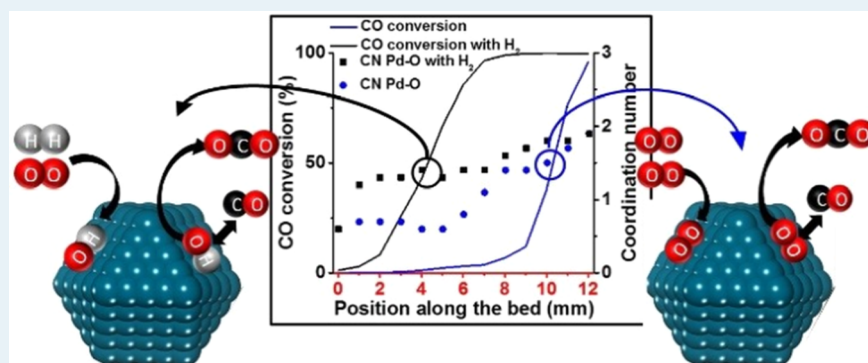
[#]Leibniz-Institut für Katalyse e.V, Universität Rostock, Albert-Einstein-Straße 29a, Rostock D-18059, Germany

[∇]Department of Chemistry, University College London, 20 Gordon Street, London WC1H 0AJ, U.K.

[&]School of Materials, University of Manchester, Manchester M13 9PL, U.K.

[○]School of Chemistry, University of Southampton, Southampton SO17 1BJ, U.K.

ⓈSupporting Information

ABSTRACT: The promotional effect of H₂ on the oxidation of CO is of topical interest, and there is debate over whether this promotion is due to either thermal or chemical effects. As yet there is no definitive consensus in the literature. Combining spatially resolved mass spectrometry and X-ray absorption spectroscopy (XAS), we observe a specific environment of the active catalyst during CO oxidation, having the same specific local coordination of the Pd in both the absence and presence of H₂. In combination with Temporal Analysis of Products (TAP), performed under isothermal conditions, a mechanistic insight into the promotional effect of H₂ was found, providing clear evidence of nonthermal effects in the hydrogen-promoted oxidation of carbon monoxide. We have identified that H₂ promotes the Langmuir−Hinshelwood mechanism, and we propose this is linked to the increased interaction of O with the Pd surface in the presence of H₂. This combination of spatially resolved MS and XAS and TAP studies has provided previously unobserved insights into the nature of this promotional effect.

**KEYWORDS:** CO oxidation, TAP, XAFS, spatially resolved, SPACI-FB

■ INTRODUCTION

To optimize heterogeneous catalytic performance, a full understanding of the correlation between structure and reactivity is required. The deficiency of such knowledge has resulted in excessive loading of precious metals in order to guarantee the desired performance.[1,2] However, this is not an economically viable methodology. Ultimately, a better understanding of catalytic processes and indeed the correlation of
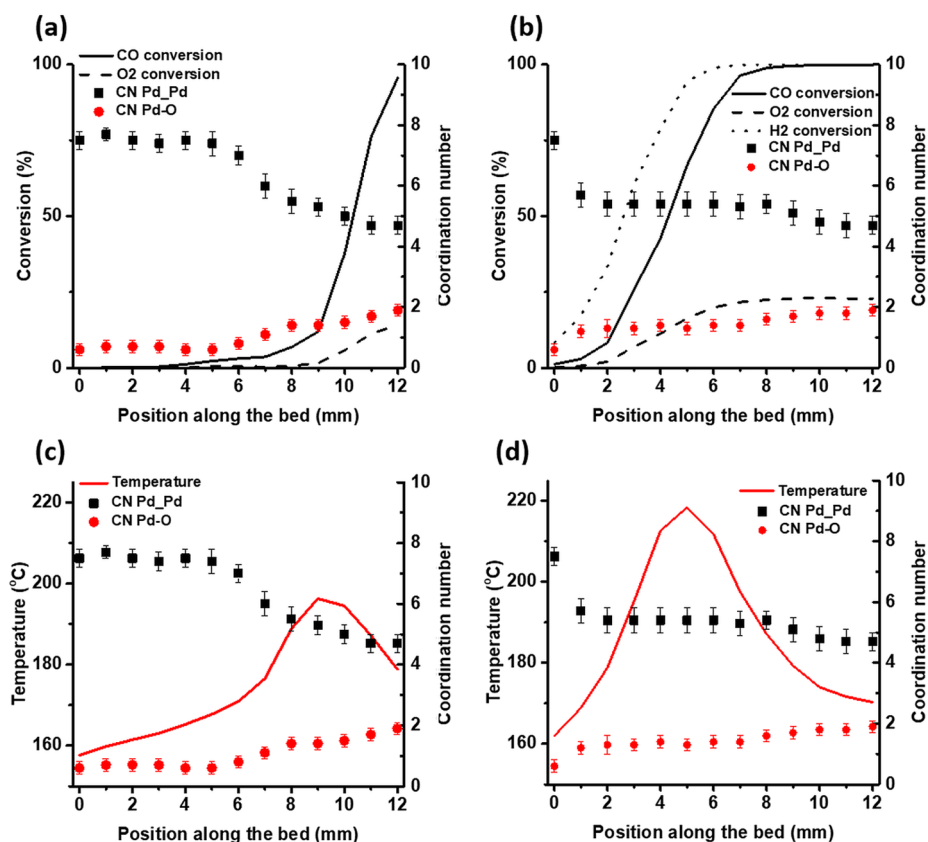
Figure 1. Variation of coordination to Pd and O and the conversion of CO, O_2, and H_2 along the length of the catalyst bed for (a) CO oxidation and (b) CO oxidation in the presence of H_2. Coordination numbers are plotted with the temperature profile for (c) CO oxidation and (d) CO oxidation in the presence of H_2.

catalyst structure and activity are required. This can be achieved via a combination of in situ catalyst characterization and kinetic measurements.[3]

The promotion of CO oxidation in the presence of hydrogen is a reaction of interest, particularly for proton-exchange membrane fuel cells (PEMFCs).[4,5] PEMFCs have high efficiency, operate at low temperature (80 °C), and are fueled by H_2 produced from steam reforming, partial oxidation, or autothermal reforming of natural gas and other liquid fuels.[6,7] As CO, even in trace amounts (1 ppm), is a poison for PEMFCs at low temperature, all CO must be removed. Large amounts of CO are initially reduced to ~1% by the water-gas shift reaction. To further reduce the concentration, CO oxidation over supported noble-metal catalysts[8] is a suitable method, showing high conversions at low temperatures. The presence of a small amount of H_2 in the feed shifts the light-off to a lower temperature, a phenomenon which has been widely reported for platinum[9−15] and gold,[16] but there are only limited observations in the case of palladium.[17,18] However, it is not well understood why the presence of hydrogen has a promotional effect on CO oxidation. There are currently two theories on this promotional effect:

(i) H_2 combustion produces heat, thereby increasing the rate of reaction for CO oxidation.[19]

(ii) H_2 promotes CO oxidation through a physico-chemical effect.[20]

There is also the possibility that both thermal and physico-chemical effects contribute in tandem to promote CO oxidation.

While thermal effects are always likely to contribute under operand oconditions, in this study the contribution of any non-thermal effects (physico-chemical) to the CO oxidation in the presence of H_2 over a Pd/Al_2O_3 catalyst is investigated. This study employed a combination of temporal analysis of products (TAP) measurements and a combined spatially resolved X-ray absorption spectroscopy (XAS) and spatially resolved mass spectrometry analysis.

In order to investigate the elementary steps of the reactions, a transient pulse response methodology was employed using a TAP reactor.[21−25] This technique has been proven to provide key insights into elementary steps of catalytic processes.[26,27] However, despite the ability to screen varying oxidation states via multi-pulse experiments,[28] TAP is not typically used to determine structure−activity correlations. TAP is, however, ideally suited to determine the role of any nonthermal effects due to operation in the Knudsen diffusion regime, owing to the use of small amounts of reactive gases.[29] In this regime gas−gas interactions are eliminated and experimental conditions maintained such that an isothermal catalyst zone is created:[30] i.e., no promotional thermal effects. The well-defined transport regime of Knudsen diffusion has allowed for the development of well-established moment based analytical methodologies,[31,32] which are utilized herein to determine conversions and residence times of gases.

As structural characterization is typically conducted with the aid of spectroscopic techniques,[33] there is a growing trend in the development of operando methods.[34−39] In addition, there has also been a development of spatially resolved methodologies to monitor the evolution of reactant concentrations,[40−43] as well as
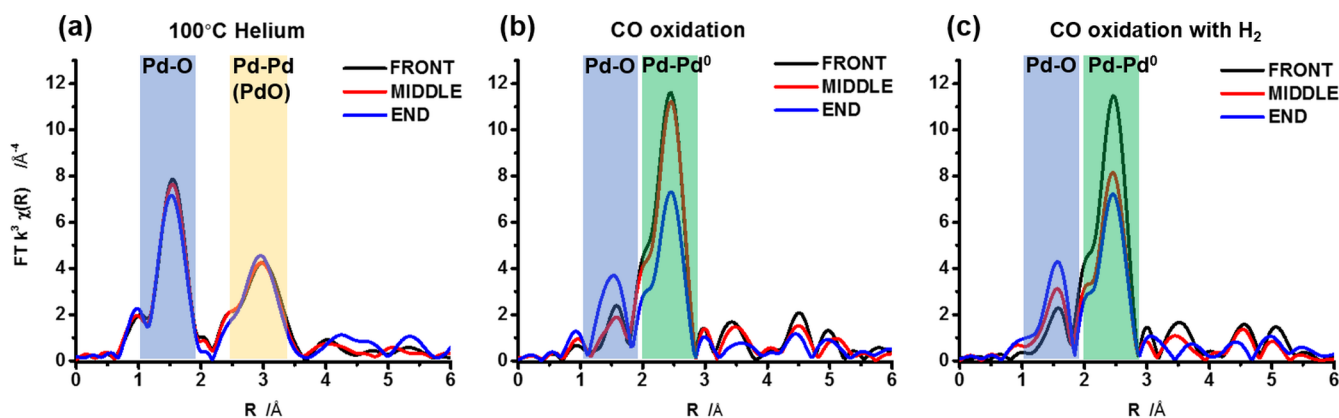
Figure 2. Magnitude component of the k^3-weighted non-phase-corrected Fourier transform of the EXAFS data at the front, middle, and end of the catalyst bed of the (a) fresh catalyst, (b) the catalyst under CO oxidation, and (c) the catalyst under CO oxidation with H_2. Features consistent with scattering from O, Pd (of Pd^0), and Pd (of PdO) are highlighted in blue, green, and yellow boxes, respectively.

significant advances in the imaging of spatial heterogeneities within catalytic reactors.[33,44,45] With this in mind, the minimally invasive SPACI-FB technique[8,46−48] has been coupled with X-ray absorption fine structure (XAFS) for the first time, providing spatially resolved correlations of gas-phase concentrations, catalyst bed temperatures, and information on the catalyst structure (via XAFS). This combination of techniques (to be known as SPACI-FB-XAFS) enables a profile of the gas-phase concentrations and temperature through a fixed catalytic bed, to be correlated to the structure of the catalyst at the same axial position in the bed. Consequently, we are able to report on the contribution of both chemical and structural effects in the promotion of CO oxidation by hydrogen.

RESULTS AND DISCUSSION

From the combined SPACI-FB-XAFS measurements we were able to correlate changes in the catalyst structure (from the coordination numbers determined from the extended X-ray absorption fine structure (EXAFS) analysis) with the reaction profile along the catalyst bed (from the MS data). These profiles are shown for CO oxidation in both the absence and presence of H_2 in Figure 1. In comparison to CO oxidation without H_2 (Figure 1a), in the presence of H_2 (Figure 1b), light-off occurs much closer to the beginning of the catalyst bed, confirming the promotional effect of H_2. As can be clearly observed from Figure 1, the structural change also occurs much earlier in the bed in the presence of H_2. It should be noted that the changes in temperature and structure (Figures 1c,d) do not follow the same trends and, therefore, are not likely to be entirely connected, indicating the likely presence of both thermal and nonthermal promotional effects. However, in both the absence and the presence of H_2, the onset of CO conversion only occurs once the Pd catalyst has reached a similar local coordination (Figure 1a,b), with coordination to O and Pd of 1.5 and 5, respectively.

These spatially resolved measurements were performed after heating the catalyst to reaction temperature under reactant gases and allowing the system to attain steady state. The EXAFS spectra collected during both reactions can be fitted to two scattering paths, an O path at 1.97 Å and a Pd path at 2.74 Å, the Pd distance being consistent with metallic Pd (highlighted in blue and green in Figures 2b,c). The Pd−Pd scattering path at 3 Å, characteristic of PdO, could not be fitted to these data, at any point along the catalyst bed; this feature is highlighted in yellow in Figure 2a. For CO oxidation both with and without H_2 the

catalyst structure is consistent with a Pd nanoparticle (NP) with coordination to an adsorbed low-Z-number element (O, CO, or OH). The fitting parameters and examples of the fits are shown in Tables S1−S3 and Figures S4−S6 in the Supporting Information.

The fresh catalyst, however, is consistent with PdO, the data fitting well to one O and two Pd scattering paths at 2.015, 3.05, and 3.44 Å, respectively. Heating the catalyst in reaction gases resulted in removal of O from the PdO structure, as a consequence of PdO reaction with the reductant gases present in the feed (CO or CO and H_2). However, during the ramp and attainment of steady state this O could not be replenished from the gas phase and so the catalyst during both reactions is a reduced Pd NP with adsorbed surface O (or other low-Z-number element).

The relative changes in catalyst structure during CO oxidation with and without H_2 are observed in Figure 2b,c. For CO oxidation without H_2 the front and middle of the bed are dominated by Pd scattering, whereas during CO oxidation with H_2 the increase in scattering from a low-Z-number element has already occurred by the middle of the bed. From a linear combination fit (LCF) of the XANES spectra we can follow the changes in the relative oxidation state of the Pd NPs during the reaction, by fitting the data to contributions of Pd^{2+} and Pd^0 (Figure 3).

The increase in Pd^{2+} contribution follows the same trend as the change in O coordination observed from the EXAFS fitting (Figures 1a and 3a). As adsorbed CO has a neutral charge and adsorbed O a 2− charge, we can therefore be confident that the increase in Pd^{2+} contribution coincides with an increase in the concentration of adsorbed O and so the low-Z-number element observed in the EXAFS analysis is coordination to adsorbed O. The fact that CO conversion only reaches 50% under CO oxidation with and without H_2 after the catalyst has attained the same local coordination (O of 1.5 and Pd of 5) would imply a certain concentration of surface O is required for reaction to occur. The difference between the two reactions is how this surface O concentration is obtained. Under CO oxidation conditions it appears that a certain temperature is required before CO oxidation occurs (see Figure 1c), starting at 165 °C (5 mm along the bed). After this temperature is reached, CO conversion increases slowly as surface O content increases. The maximum rate of change of structure of the Pd nanoparticles occurs as the exotherm reaches a maximum at 195 °C. We
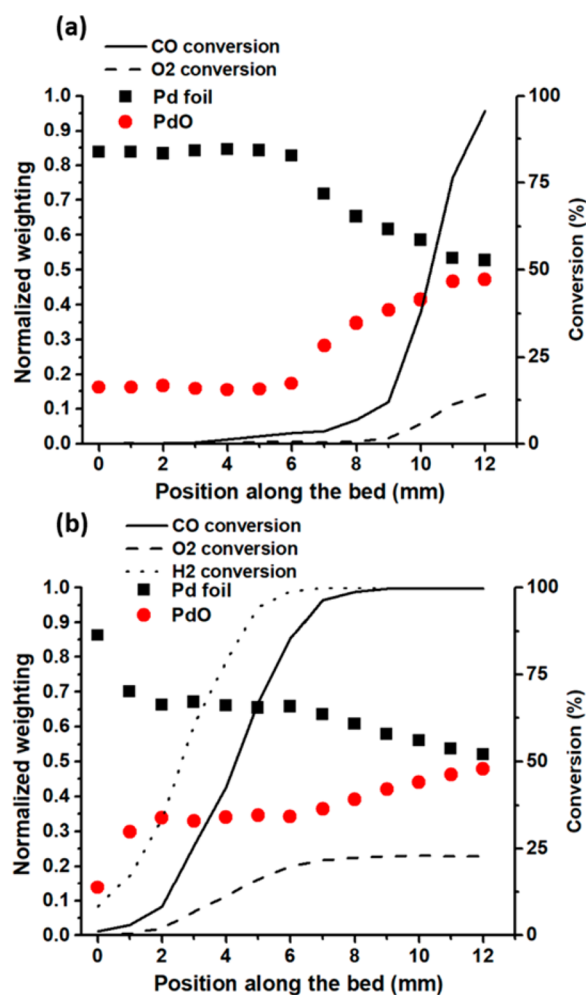
Figure 3. Relative contributions of a Pd metal standard and PdO as a function of position in the catalyst bed during (a) CO oxidation and (b) CO oxidation with H_2.

propose that an initial small amount of CO conversion results in a small localized increase in temperature, thus enabling more CO to react and desorb, leaving more sites available for O adsorption. This results in an autocatalytic type change to the surface coverage, as previously observed for CO oxidation using XPS.[49]

Under CO oxidation in the presence of H_2, an initial increase in surface O content is observed very early in the catalyst bed, which coincides with H_2 consumption. This early change in structure is thought to occur through a promotional effect of H_2 or hydroxyls on the Pd surface. It could be envisioned that dissociatively adsorbed H_2 on the Pd surface can react with O_2 to produce adsorbed hydroxyl species, with which CO can more easily react than with oxygen. Although from this combined SPACI-FB-XAFS study we have no direct evidence of the presence of OH species, the promotional effect of hydroxyls has previously been investigated using a variety of techniques such as XPS, inelastic neutron scattering (INS), and isotopic exchange experiments.[50−52] From XPS and catalytic activity studies comparing anhydrous and hydrous PdO, only the latter was found to be active and the water of hydration was found to be in the form of OH groups. These authors proposed two roles for the OH species: the oxidation of CO by OH and the formation of PdO through the formation of water from reaction of two OH groups.[50] Direct evidence for the involvement of OH species in

CO oxidation is shown in the INS study, where a decrease in the Pd−OH hydroxyl band intensity at 900 cm^{-1} was observed on reaction.[51] Further evidence of the role of OH groups comes from an isotopically labeled O_2 study, used to investigate a Pd/Al_2O_3 catalyst during CO and propene oxidation.[52] In that work, the oxidation of CO was found to be due to interaction with OH species and not from reaction with O_2.[52] The current work would suggest a Langmuir−Hinshelwood mechanism, where the reaction is dependent on the coverage of surface species. CO conversion reaches 50% at ∼5 mm into the catalyst bed, at which point the structure has reached the same coordination as observed in CO oxidation (without H_2). However, from the LCF of the XANES data (Figure 3) it is clear that the average oxidation state at 50% CO conversion (5 mm) is different from that observed during CO oxidation (without H_2) (10 mm). The contribution of Pd^{2+} is less under CO oxidation with H_2 than without H_2, which could be linked to the adsorption of other types of species, potentially hydroxyls.

It should be noted that even at the end of the catalyst bed under both sets of reaction conditions, where all the CO (and H_2) has been consumed, the catalyst does not re-oxidize to form a bulk PdO structure. The temperatures reached in the catalyst bed are not sufficient for a complete re-oxidation of the catalyst, requiring temperatures typically over 200 °C for bulk oxidation to start.[53]

TAP experiments were conducted, providing further insight into the CO oxidation with and without H_2 from both a mechanistic and kinetic point of view. For the latter purpose, the TAP data were treated according to the moment based analysis and basic kinetic coefficient methods.[54] From the obtained values of adsorption rate constant k_a of CO for the experiments without H_2 (2.36 s^{-1}) and with H_2 (1.13 s^{-1}), it is clear that CO adsorbs more slowly in the presence of H_2, which would indicate that there is some competition for adsorption sites between CO and H_2. When CO oxidation is performed over the pre-reduced or pre-oxidized catalyst, a clear increase in CO conversion for the former material is observed: i.e., 99% over the pre-reduced catalyst in comparison to 71% conversion for the pre-oxidized catalyst (Figure 4a). This would imply that the presence of Pd, most likely present in the prereduced catalyst, promotes activity. This is consistent with the XAFS data, which showed that the catalyst was already in a reduced state prior to reaction both with and without H_2. PdO appears to be less able to convert CO to CO_2, i.e. provide O, and from the XAFS results we propose that a certain coverage of adsorbed oxygen species (in the case of CO oxidation) is required for conversion. This indicates the presence of a Langmuir−Hinshelwood type mechanism over the Pd NPs which is promoted in the presence of H_2.

In order to identify the kind of oxygen species participating in CO oxidation to CO_2, TAP experiments were conducted in the presence and absence of H_2. The surface of the catalyst was pretreated with $^{16}O_2$ and then subjected to sequential pulses of $C^{16}O$ and $^{18}O_2$. $^{16}CO_2$ was the main carbon dioxide isotope upon CO oxidation in the absence of H_2, thus proving that strongly adsorbed ^{16}O species (formed upon catalyst pretreatment) participated in the oxidation reaction (Figure 4b). When H_2 was in the reaction feed, a greater contribution of ^{18}O-containing carbon dioxide was observed. To check if H_2 simply promotes an oxygen isotopic exchange between $C^{16}O_2$ and $^{18}O_2$, these components were pulsed together over the catalyst at 200 °C following an $^{16}O_2$ pre-treatment at 300 °C. No $^{18}CO_2$ and only small amounts of $C^{18}O^{16}O$ were detected (less than a 10% fraction (Figure S7)) in comparison to 50% $C^{18}O^{16}O$ formed
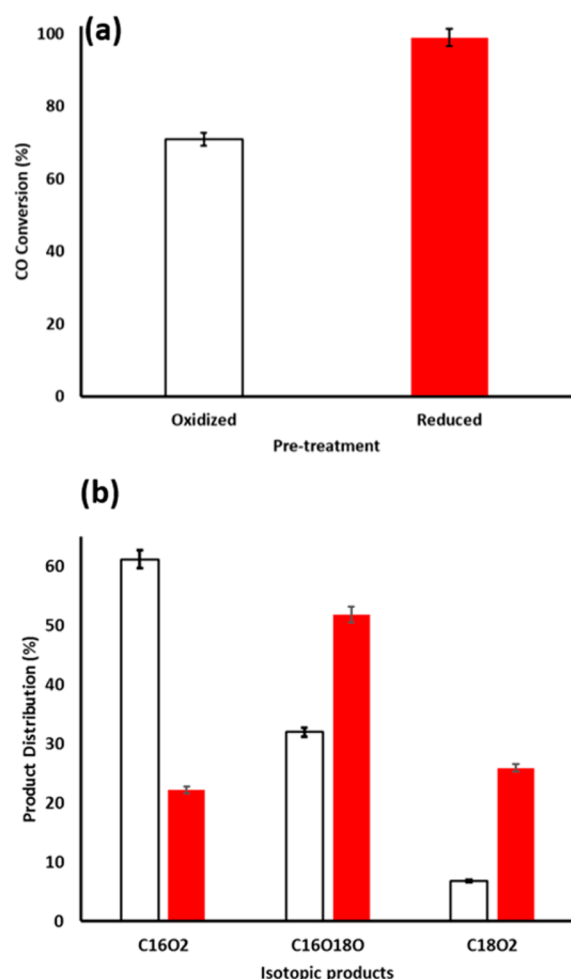
Figure 4. CO conversion (a) upon pulsing an $^{18}O_2$:CO:Ar = 1:1:2 mixture over pre-oxidized (white) and pre-reduced (red) Pd/Al_2O_3 at 200 °C. (b) Product distributions of $C^{16}O_2$, $C^{16}O^{18}O$, and $C^{18}O_2$ for CO oxidation upon pulsing an $^{18}O_2$:CO:Ar = 1:1:2 mixture (white) and CO oxidation upon sequential pulsing of H_2:Ne = 1:1 and $^{18}O_2$:CO:Ar = 1:1:2 mixtures with a time delay of 0.1 s (red) over the preoxidized catalyst.

upon CO oxidation (Figure 4). Therefore, isotopically labeled carbon dioxide in the $^{18}O_2/C^{16}O/H_2$ test originated through a reaction of $C^{16}O$ with short-lived ^{18}O-containing species formed from $^{18}O_2$. Such a species could be ^{18}OH when the XAFS measurements are considered, where the promotional effect of H_2 is proposed to occur through the formation of surface OHs. An additional support for the presence of this surface species is the experimental residence time (derived from 1st moment, M_1) of H_2, which was 0.39 s and indicates a significant interaction with the catalyst. This could be due to OH formation, considering that the theoretical Knudsen diffusional residence time is 0.065 s (derived from the analogous argon first moment and the known linear dependence of Knudsen diffusion on molecular weight and temperature).[55] In the absence of H_2, where there is no formation of OHs, the oxidation of CO appears to proceed via reaction with strongly adsorbed ^{16}O, with the majority of product being $C^{16}O_2$.

To summarize, the major outcomes from this reported work are as follows:

(1) This is the first reported instance of a simultaneous, spatially resolved gas concentration, catalyst temperature,

and XAFS study using the SPACI-FB method, to be known as SPACI-FB-XAFS.

(2) There are nonthermal effects occurring in the hydrogen-promoted oxidation of carbon monoxide, as evidenced from the structural changes from XAFS and the presence of promotional effects under TAP conditions. It should be noted that thermal effects may also have an influence on the observed promotion of the reaction.

(3) CO oxidation is observed both in the presence and absence of H_2 once the same local coordination of the Pd NPs (coordination to O and Pd of 1.5 and 5, respectively) has been reached.

(4) There is a competitive adsorption between hydrogen and carbon monoxide, as evidenced in TAP results by the slowing of the rate of adsorption of carbon monoxide in the presence of hydrogen.

(5) There is a significant interaction of hydrogen with the catalyst surface (TAP 1st moment data).

(6) The presence of hydrogen has in fact promoted the Langmuir–Hinshelwood mechanism.

CONCLUSIONS

From this combination of TAP reactor studies and spatially resolved SPACI-FB-XAFS measurements, we conclude that the H_2 promotion on CO oxidation over Pd/Al_2O_3 proceeds through a physico-chemical effect. During CO oxidation in both the absence and presence of H_2 the catalyst structure is consistent with a Pd nanoparticle with adsorbed surface O, with a specific surface concentration of O (or OHs) which appears to be required before light-off is observed. In the presence of hydrogen the activation of the catalyst occurs at a place closer to the front end of the bed, most likely via the reaction of H_2 and gas-phase O_2 to form adsorbed OHs, which from previous studies have been shown to more readily react with CO in comparison to surface O. TAP reactor studies confirm the presence of a nonthermal effect and, through O-isotopic experiments, confirm the increased interaction of gas-phase O_2 on CO oxidation with H_2 in comparison to CO oxidation in the absence of H_2. We propose that this is due to the formation of surface hydroxyls in the presence of H_2, which then preferentially react with CO over adsorbed O.

The ability to show that the activation of the catalyst shifts in the catalyst bed and to correlate with the gas-phase products and thus catalyst conversion demonstrates the strength of this combination of techniques. Our results show that the structure evidently changes through the bed and, crucially, during the actual reaction. This allows for a clearer picture of the overall catalyst performance via SPACI-FB-XAFS, information which, to our knowledge, has not been reported previously.

EXPERIMENTAL METHODS

Catalyst Preparation. The 1 wt % Pd/Al_2O_3 catalyst used in this work was prepared by wetness impregnation of γ-Al_2O_3 (Alfa Aesar, SA = 232 m^2/g). The Al_2O_3 support was ground to a particle size of <150 μm and mixed with an aqueous solution containing $Pd(NO_3)_2$. The mixture was vigorously stirred and heated to 60 °C for 4 h until the excess amount of water was removed and the mixture became a slurry. The catalyst was then dried at 110 °C overnight, after which the catalyst was calcined at 550 °C for 4–6 h. The fresh catalyst was characterized by powder X-ray diffraction and TEM. These results are shown in Figures S1–S3 of the Supporting Information.
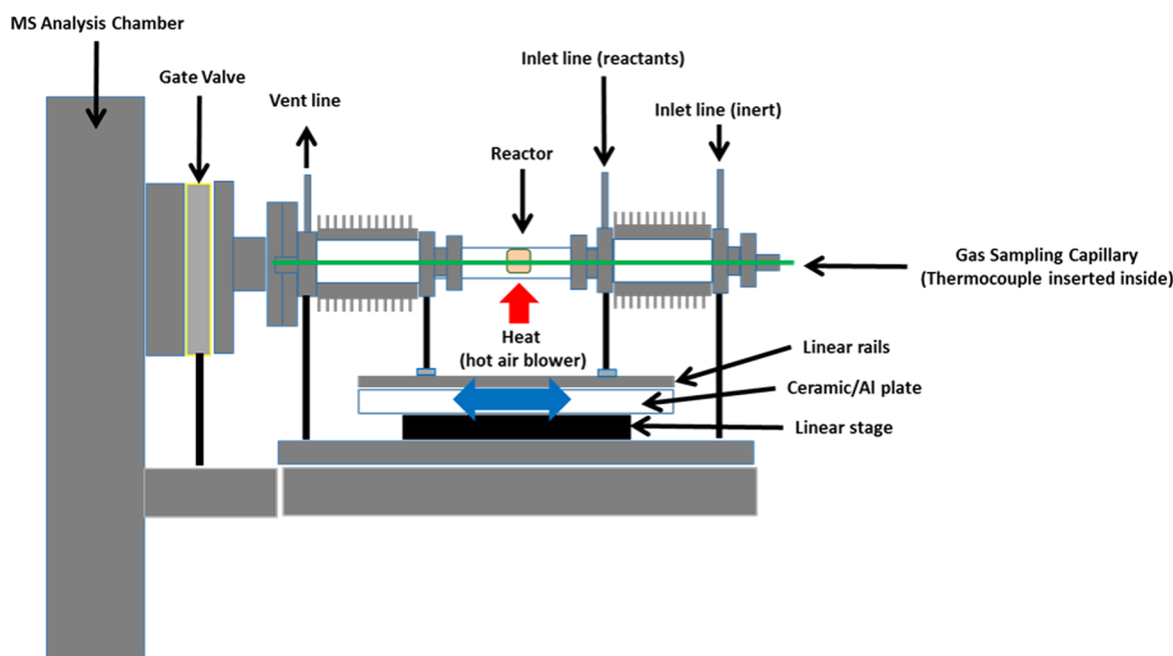
Figure 5. Schematic of the SPACI-FB equipment.

SPACI-FB-XAFS Experiments. Figure 5 is a schematic of the SPACI-FB system, while Figure 6 is a photograph of the
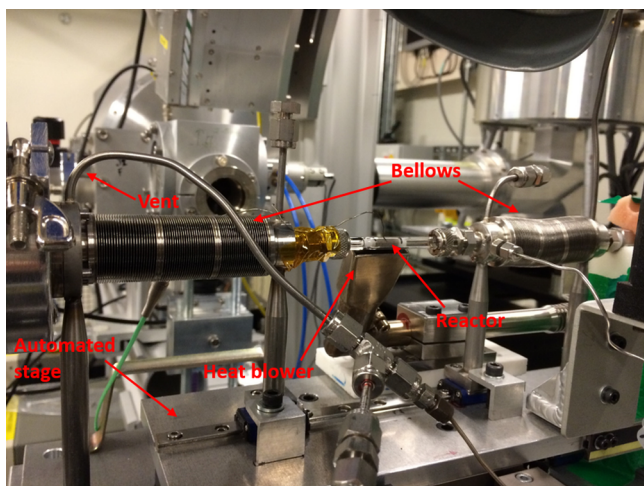

Figure 6. SPACI-FB equipment on beamline B18 at the Diamond Light Source.

experimental setup in place on B18 at the Diamond Light Source, UK. Further experimental setup details of the SPACI-FB-XAFS system are reported elsewhere.[48] Critically, precise alignment of the X-ray beam, the thermocouple, and holes in wall of the sampling capillary is required in order to ensure that coincident measurements are examining the same part of the catalyst bed. This was achieved through laser alignment and micrometer precision stages. A quartz reactor was used to hold the catalyst which the X-rays passed through to measure the Pd K edge transmission XAFS data. A catalyst bed length of 12 mm was utilized, and the data points (gas composition and XAFS) were collected over 15 min every 1 mm of the reactor to obtain sufficient signal to noise and spatial resolution. The XAFS experimental details are provided in the Supporting Information. The SPACI-FB experimental method is similar to the method

outlined in previous publications.[8] The O_2:CO ratio was 3:1, 3% O_2, 1% CO, 10% Ar, with and without 0.6% H_2, total flow 100 mL min^{-1}, He as a balance gas. Steady-state conditions were ensured by allowing the system to equilibrate for 1 h prior to any measurements, and a comparison of measurements was made at the same axial position at different time points. XAFS data processing was performed using IFEFFIT with the Horae package (Athena and Artemis).[56,57] The fitting parameters are shown in Tables S1−S3 in the Supporting Information.

TAP Experiments. An ultrahigh-vacuum (UHV) TAP-2 system was utilized for this study.[21−25,58] In this setup, pulse valves are at atmospheric pressure with the outlet of the quartz microreactor (i.d. 6 mm, length 40 mm) in direct contact with the UHV analysis chamber, where the exit flow is analyzed by a quadrupole mass spectrometer (Hiden HAL RC 301). The Pd/Al_2O_3 catalyst (20 mg) was packed between two layers of quartz (sieve fraction of 250−355 μm) within the isothermal zone of a quartz tube microreactor. Before transient experiments the catalyst was pretreated at 300 °C in a flow of 16 mL min^{-1} N_2 with 4 mL min^{-1} O_2 (oxidized) or H_2 (reduced) for 0.5 h. Hereafter, the reactor was exposed to vacuum (10^{-5} Pa) with a simultaneous decrease of temperature to 200 °C unless otherwise stated. CO:Ar = 1:1, $^{18}O_2$:CO:Ar = 1:1:2, H_2:Ne = 1:1, CO_2:Ar = 1:1, and $^{18}O_2$:Ne = 1:1 mixtures were used in these experiments. The reaction mixtures were prepared using O_2 (Air Liquide 5.5), $^{18}O_2$ (CAMPRO scientific, 97% ^{18}O), CO (Linde, 3.7), CO_2 (Linde, 4.5), H_2 (Air Liquide, 5.0), Ar (5.0), and Ne (Linde, 5.0) without additional purification. The following atomic mass units were used for mass spectrometric identification of different compounds: 48 ($C^{18}O_2$), 46 ($C^{18}O^{16}O$), 44 ($^{16}CO_2$), 36 ($^{18}O_2$), 34 ($^{18}O^{16}O$), 32 ($^{16}O_2$), 30 ($C^{18}O$, $C^{18}O^{16}O$), 28 ($C^{16}O$, $C^{16}O_2$), 18 (H_2O), 2 (H_2), 20 (Ne), and 40 (Ar). Operation within the Knudsen diffusion regime (and by extension isothermal conditions), which is essential for TAP moment based analysis,[54,55] was also confirmed via comparison of inert gas (argon) experimental pulse response with theoretical Knudsen diffusion pulse response for argon.

The data were analyzed using the well-established moment based approach,[54] and reported results are derived from the averages of three experimental data sets, each one consisting of 200 pulses.

■ ASSOCIATED CONTENT

Ⓢ Supporting Information

The Supporting Information is available free of charge on the ACS Publications website at DOI: 10.1021/acscatal.8b01509.

> EXAFS analysis, results of the linear combination fit of the XANES, and equations relating to the TAP analysis (PDF)
>
> The XAFS spectra, TAP data, mass spectrometry files, TEM and XRD data underpinning the results shown in the manuscript can be accessed from the University of Glasgow and Queen's University Belfast's data repositories: http://dx.doi.org/10.5525/gla.researchdata.654 and https://doi.org/10.17034/e97ee975-90e2-41f8-b28a-1ae1438dcb91.

■ AUTHOR INFORMATION

Corresponding Authors
*E-mail for E.K.G.: emma.gibson@glasgow.ac.uk.
*E-mail for K.M.: kmorgan08@qub.ac.uk.

ORCID Ⓞ
Emma K. Gibson: 0000-0002-7839-3786
Kevin Morgan: 0000-0002-6648-2546
Christopher Hardacre: 0000-0001-7256-6765
Sarah J. Haigh: 0000-0001-5509-6706

Notes
The authors declare no competing financial interest.

■ ACKNOWLEDGMENTS

■ REFERENCES

(1) Hageluken, C. Recycling the Platinum Group Metals: A European Perspective. *Platinum Met. Rev.* **2012**, *56*, 29−35.

(2) Morgan, K.; Goguet, A.; Hardacre, C. Metal Redispersion Strategies for Recycling of Supported Metal Catalysts: A Perspective. *ACS Catal.* **2015**, *5*, 3430−3445.

(3) Morgan, K.; Touitou, J.; Choi, J. S.; Coney, C.; Hardacre, C.; Pihl, J. A.; Stere, C. E.; Kim, M. Y.; Stewart, C.; Goguet, A.; Partridge, W. P. Evolution and Enabling Capabilities of Spatially Resolved Techniques for the Characterization of Heterogeneously Catalyzed Reactions. *ACS Catal.* **2016**, *6*, 1356−1381.

(4) Lopes, P. P.; Freitas, K. S.; Ticianelli, E. A. CO Tolerance of PEMFC Anodes: Mechanisms and Electrode Designs. *Electrocatalysis* **2010**, *1*, 200−212.

(5) Qwabe, L. Q.; Dasireddy, V. D. B. C.; Singh, S.; Friedrich, H. B. Preferential CO oxidation in a hydrogen-rich stream over gold supported on Ni−Fe mixed metal oxides for fuel cell applications. *Int. J. Hydrogen Energy* **2016**, *41*, 2144−2153.

(6) Armor, J. N. The multiple roles for catalysis in the production of H_2. *Appl. Catal., A* **1999**, *176*, 159−176.

(7) Aupretre, F.; Descombe, C.; Duprez, D. Bio-ethanol catalytic steam reforming over supported metal catalysts. *Catal. Commun.* **2002**, *3*, 263−267.

(8) Touitou, J.; Morgan, K.; Burch, R.; Hardacre, C.; Goguet, A. An in situ spatially resolved method to probe gas phase reactions through a fixed bed catalyst. *Catal. Sci. Technol.* **2012**, *2*, 1811−1813.

(9) Dabill, D. W.; Gentry, S. J.; Holland, H. B.; Jones, A. The oxidation of hydrogen and carbon monoxide mixtures over platinum. *J. Catal.* **1978**, *53*, 164−167.

(10) Kahlich, M. J.; Gasteiger, H. A.; Behm, R. J. Kinetics of the Selective CO Oxidation in H2-Rich Gas on Pt/Al2O3. *J. Catal.* **1997**, *171*, 93−105.

(11) Salomons, S.; Votsmeier, M.; Hayes, R. E.; Drochner, A.; Vogel, H.; Gieshoff, J. CO and H_2 oxidation on a platinum monolith diesel oxidation catalyst. *Catal. Today* **2006**, *117*, 491−497.

(12) Hauptmann, W.; Votsmeier, M.; Hayes, R. E.; Vlachos, D. G. Modelling the simultaneous oxidation of CO and H_2 on Pt- Promoting effect on H2 on the CO light-off. *Appl. Catal., A* **2011**, *397*, 174−182.

(13) Daté, M.; Okumura, M.; Tsubota, S.; Haruta, M. Vital Role of Moisture in the Catalytic Activity of Supported Gold Nanoparticles. *Angew. Chem., Int. Ed.* **2004**, *43*, 2129−2132.

(14) Sun, M.; Croiset, E. B.; Hudgins, R. R.; Silveston, P. L.; Menzinger, M. Multiplicity and Superadiabatic Extinction Waves in the Oxidation of CO/H_2 Mixtures over a Pt/Al2O3-Coated Monolith. *Ind. Eng. Chem. Res.* **2002**, *42*, 37−45.

(15) Zheng, X.; Schultze, M.; Mantzaras, J.; Bombach, R. Effects of hydrogen addition on the catalytic oxidation of carbon monoxide over platinum at power generation relevant temperatures. *Proc. Combust. Inst.* **2013**, *34*, 3343−3350.

(16) Rossignol, C.; Arrii, S.; Morfin, F.; Piccolo, L.; Caps, V.; Rousset, J. L. Selective oxidation of CO over model gold-based catalysts in the presence of H_2. *J. Catal.* **2005**, *230*, 476−483.

(17) Baddour, R. F.; Modell, M.; Goldsmith, R. L. The palladium-catalyzed carbon monoxide oxidation. Catalyst "break-in" phenomen-on,. *J. Phys. Chem.* **1970**, *74*, 1787−1796.

(18) Goldsmith, R. L.; Modell, M.; Baddour, R. F. Hydrogen promotion of the palladium-catalysed carbon monoxide oxidation. *J. Phys. Chem.* **1971**, *75*, 2065−2066.

(19) Sun, M.; Croiset, E. B.; Hudgins, R. R.; Silveston, P. L. Steady-State Multiplicity and Superadiabatic Extinction Waves in the Oxidation of CO/H_2 Mixtures over a Pt/Al2O3-Coated Monolith. *Ind. Eng. Chem. Res.* **2003**, *42*, 37−45.

(20) Piccolo, L.; Daly, H.; Valcarcel, A.; Meunier, F. C. Promotional effect of H_2 on CO oxidation over Au/TiO2 studied by operando infrared spectroscopy. *Appl. Catal., B* **2009**, *86*, 190−195.

(21) Gleaves, J. T.; Ebner, J. R.; Kuechler, T. C. Temporal Analysis of Products (TAP)—A Unique Catalyst Evaluation System with Submillisecond Time Resolution. *Catal. Rev.: Sci. Eng.* **1988**, *30*, 49−116.

(22) Pérez-Ramírez, J.; Kondratenko, E. V. Evolution, achievements, and perspectives of the TAP technique. *Catal. Today* **2007**, *121*, 160−169.

(23) Hinrichsen, O.; van Veen, A. C.; Zanthoff, H. W.; Muhler, M. In *TAP Reactor Studies in In Situ Spectroscopy in Heterogeneous Catalysis*; Haw, J. F., Ed.; Wiley-VCH: Weinheim, Germany, 2002; pp 237−269.

(24) Gleaves, J. T.; Yablonsky, G.; Zheng, X.; Fushimi, R.; Mills, P. L. Temporal analysis of products (TAP)—Recent advances in technology for kinetic analysis of multi-component catalysts. *J. Mol. Catal. A: Chem.* **2010**, *315*, 108−134.

(25) Morgan, K.; Maguire, N.; Fushimi, R.; Gleaves, J. T.; Goguet, A.; Harold, M. P.; Kondratenko, E. V.; Menon, U.; Schuurman, Y.; Yablonsky, G. S. *Catal. Sci. Technol.* **2017**, *7*, 2416−2439.

(26) Pérez-Ramírez, J.; Kondratenko, E. V.; Novell-Leruth, G.; Ricar, J. M. Mechanism of ammonia oxidation over PGM (Pt, Pd, Rh) wires by temporal analysis of products and density functional theory. *J. Catal.* **2009**, *261*, 217−223.

(27) Kondratenko, V. A. Mechanistic analysis of oxygen-assisted coupling of methane and ammonia to hydrogen cyanide over polycrystalline Pt and Rh. *Catal. Sci. Technol.* **2015**, *5*, 1598.

(28) Kondratenko, E. V.; Wang, H.; Kondratenko, V. A.; Caro, J. Selective oxidation of CH_4 and C_2H_6 over a mixed oxygen ion and electron conducting perovskite—A TAP and membrane reactors study. *J. Mol. Catal. A: Chem.* **2009**, *297*, 142−149.

(29) Schuurman, Y. Assessment of kinetic modeling procedures of TAP experiments. *Catal. Today* **2007**, *121*, 187−196.

(30) Goguet, A.; Hardacre, C.; Inceesungvorn, B.; Morgan, K.; Shekhtman, S. O. Correction for a possible reversible adsorption over an ″inert″ material. *Catal. Sci. Technol.* **2011**, *1*, 760−767.

(31) Morgan, K.; Inceesungvorn, B.; Goguet, A.; Hardacre, C.; Meunier, F. C.; Shekhtman, S. O. TAP studies on 2% Ag/γ-Al₂O₃ catalyst for selective reduction of oxygen in a H₂ rich ethylene feed. *Catal. Sci. Technol.* **2012**, *2*, 2128−2133.

(32) Morgan, K.; Goguet, A.; Hardacre, C.; Kondratenko, E. V.; McManus, C.; Shekhtman, S. O. Expansion of pulse responses from temporal analysis of products (TAP) pulse responses for more accurate data analysis. *Catal. Sci. Technol.* **2014**, *4*, 3665−3671.

(33) Beale, A. M.; Jacques, S. D. M.; Gibson, E. K.; Di Michiel, M. Progress towards five dimensional diffraction imaging of functional materials under process conditions. *Coord. Chem. Rev.* **2014**, *277-278*, 208−223.

(34) Geantet, C.; Pichon, C. In *X-Ray Absorption Spectroscopy in Characterization of Solid Materials and Heterogeneous Catalysts: From Structure to Surface Reactivity*; Che, M., Védrine, J. C., Eds.; Wiley-VCH: Weinheim, Germany, 2012; Vol. *1*, pp 511−536.

(35) Safonova, O.; Deniau, B.; Millet, J. M. M. Mechanism of the Oxidation−Reduction of the MoVSbNbO Catalyst: In Operando X-ray Absorption Spectros-copy and Electrical Conductivity Measure-ments. *J. Phys. Chem. B* **2006**, *110*, 23962−23967.

(36) Bentrup, U. Combining in situ characterization methods in one set-up: looking with more eyes into the intricate chemistry of the synthesis and working of heterogeneous catalysts. *Chem. Soc. Rev.* **2010**, *39*, 4718−4730.

(37) Thibault-Starzyk, F.; Maugé, F. In *Infrared Spectroscopy in Characterization of Solid Materials and Heterogeneous Catalysts: From Structure to Surface Reactivity*; Che, M., Védrine, J. C., Eds.; Wiley-VCH: Weinheim, Germany, 2012; Vol. *1*, 1−48.

(38) Behrens, M.; Schlögl, R. In *X-Ray Diffraction and Small Angle X-Ray Scattering in Characterization of Solid Materials and Heterogeneous Catalysts: From Structure to Surface Reactivity*; Che, M., Védrine, J. C., Eds.; Wiley-VCH: Weinheim, Germany, 2012; Vol. *2*, pp 609−653.

(39) Brant, W. R.; Li, D.; Gu, Q.; Schmid, S. Comparative analysis of ex-situ and operando X-ray diffraction experiments for lithium insertion materials. *J. Power Sources* **2016**, *302*, 126−134.

(40) Partridge, W. P.; Storey, J. M. E.; Lewis, S. A.; Smithwick, R. W.; DeVault, G. L.; Cunningham, M. J.; Currier, N. V.; Yonushonis, T. M. Time-Resolved Measurements of Emission Transients By Mass Spectrometry. *SAE Tech. Pap. Ser.* **2000**, 2000-01-2952.

(41) Sá, J.; Abreu Fernandes, D. L.; Aiouache, F.; Goguet, A.; Hardacre, C.; Lundie, D.; Naeem, W. SpaciMS: spatial and temporal operando resolution of reactions within catalytic monoliths. *Analyst* **2010**, *135*, 2260−2272.

(42) Horn, R.; Korup, O.; Geske, M.; Zavyalova, U.; Oprea, I.; Schlogl, R. Reactor for in situ measurements of spatially resolved kinetic data in heterogeneous catalysis. *Rev. Sci. Instrum.* **2010**, *81*, 064102−064109.

(43) Geske, M.; Korup, O.; Horn, R. Resolving kinetics and dynamics of a catalytic reaction inside a fixed bed reactor by combined kinetic and spectroscopic profiling. *Catal. Sci. Technol.* **2013**, *3*, 169−175.

(44) Weckhuysen, B. M. Chemical Imaging of Spatial Heterogeneities in Catalytic Solids at Different Length and Time Scales. *Angew. Chem., Int. Ed.* **2009**, *48*, 4910−4943.

(45) Buurmans, I. L. C.; Weckhuysen, B. M. Heterogeneities of individual catalyst particles in space and time as monitored by spectroscopy. *Nat. Chem.* **2012**, *4*, 873−886.

(46) Touitou, J.; Burch, R.; Hardacre, C.; McManus, C.; Morgan, K.; Sá, J.; Goguet, A. An in situ spatially resolved analytical technique to simultaneously probe gas phase reactions and temperature within the packed bed of a plug flow reactor. *Analyst* **2013**, *138*, 2858−2862.

(47) Touitou, J.; Aiouache, F.; Burch, R.; Douglas, R.; Hardacre, C.; Morgan, K.; Sá, J.; Stewart, C.; Stewart, J.; Goguet, A. Evaluation of an in situ spatial resolution instrument for fixed beds through the assessment of the invasiveness of probes and a comparison with a micro-kinetic model. *J. Catal.* **2014**, *319*, 239−246.

(48) Goguet, A.; Stewart, C.; Touitou, J.; Morgan, K. In Situ Spatially Resolved Techniques for the Investigation of Packed Bed Catalytic Reactors: Current Status and Future Outlook of Spaci-FB. *Adv. Chem. Eng.* **2017**, *50*, 131−160.

(49) Bowker, M. Automotive catalysis studied by surface science. *Chem. Soc. Rev.* **2008**, *37*, 2204−2211.

(50) Oh, S.-H.; Hoflund, G. B. Low-temperature catalytic carbon monoxide oxidation over hydrous and anhydrous palladium oxide powders. *J. Catal.* **2007**, *245*, 35−44.

(51) Parker, S. F. The role of hydroxyl groups in low temperature carbon monoxide oxidation. *Chem. Commun.* **2011**, *47*, 1988−1990.

(52) Caporali, R.; Chansai, S.; Burch, R.; Delgado, J. J.; Goguet, A.; Hardacre, C.; Mantarosie, L.; Thompsett, D. Critical role of water in the direct oxidation of CO and hydrocarbons in diesel exhaust after treatment catalysis. *Appl. Catal., B* **2014**, *147*, 764−769.

(53) Su, S. C.; Carstens, J. N.; Bell, A. T. A Study of the Dynamics of Pd Oxidation and PdO Reduction by H₂ and CH₄. *J. Catal.* **1998**, *176*, 125−135.

(54) Shekhtman, S. O.; Yablonsky, G. S.; Gleaves, J. T.; Fushimi, R. State defining″ experiment in chemical kinetics—primary character-ization of catalyst activity in a TAP experiment. *Chem. Eng. Sci.* **2003**, *58*, 4843−4859.

(55) Goguet, A.; Hardacre, C.; Maguire, N.; Morgan, K.; Shekhtman, S. O.; Thompson, S. P. Time of flight mass spectrometry for quantitative data analysis in fast transient studies using a Temporal Analysis of Products (TAP) reactor. *Analyst* **2011**, *136*, 155−163.

(56) Newville, M. IFEFFIT: interactive XAFS analysis and FEFF fitting. *J. Synchrotron Radiat.* **2001**, *8*, 322−324.

(57) Ravel, B.; Newville, M. ATHENA, ARTEMIS, HEPHAESTUS: data analysis for X-ray absorption spectroscopy using IFEFFIT. *J. Synchrotron Radiat.* **2005**, *12*, 537−541.

(58) Mavlyankariev, S. A.; Ahlers, S. J.; Kondratenko, V. A.; Linke, D.; Kondratenko, E. V. Effect of Support and Promoter on Activity and Selectivity of Gold Nanoparticles in Propanol Synthesis from CO₂, C₂H₄, and H₂. *ACS Catal.* **2016**, *6*, 3317−3325.